[CANCER RESEARCH 63, 2454–2461, May 15, 2003]

Synergistic Down-Regulation of Urokinase Plasminogen Activator Receptor and Matrix Metalloproteinase-9 in SNB19 Glioblastoma Cells Efficiently Inhibits Glioma Cell Invasion, Angiogenesis, and Tumor Growth[1]

Sajani S. Lakka, Christopher S. Gondi, Niranjan Yanamandra, Dzung H. Dinh, William C. Olivero, Meena Gujrati, and Jasti S. Rao[2]

Division of Cancer Biology, Departments of Biomedical and Therapeutic Sciences [S. S. L., C. S. G., N. Y., and J. S. R.], Neurosurgery [D. H. D., W. C. O., and J. S. R.], and Pathology [M. G.], The University of Illinois College of Medicine at Peoria, Peoria, Illinois 61656

ABSTRACT

The binding of urokinase plasminogen activator (uPA) to its receptor (uPAR) initiates a proteolytic cascade facilitating the activation of matrix metalloproteinase-9 (MMP-9), which in turn degrades the extracellular matrix. These processes have an established role in tumor invasion and metastasis. Our previous work revealed an inverse association between glioma invasion and the expression of uPAR and MMP-9. In the present study, we used the adenovirus serotype 5 vector system to generate a replication-deficient recombinant adenovirus capable of simultaneously expressing antisense uPAR and antisense MMP-9 (Ad-uPAR-MMP-9). This adenoviral construct is driven by the independent promoter elements cytomegalovirus and bovine growth hormone and SV40 polyadenylation signals to down-regulate key steps in the proteolytic cascade. Ad-uPAR-MMP-9 infection of SNB19 cells significantly decreased uPAR and MMP-9 expression as determined by immunohistochemical and Western blotting analyses. A Matrigel invasion assay revealed marked reduction in the invasiveness of the Ad-uPAR-MMP-9-infected cells compared with parental and vector controls. Tumor spheroids infected with Ad-uPAR-MMP-9 and cocultured with fetal rat brain aggregates did not invade rat brain aggregates, whereas 90–95% of the mock and empty vector-infected cells invaded the rat brain aggregates. Intracranial injection of SNB19 cells infected *ex vivo* with the Ad-uPAR-MMP-9 antisense bicistronic construct showed decreased invasiveness and tumorigenicity. s.c. injections of the bicistronic antisense construct into established tumors (U87 MG) caused tumor regression. These results support the therapeutic potential of targeting the individual components of the uPAR-MMP-9 by using a single adenovirus construct for the treatment of gliomas and other cancers.

INTRODUCTION

Tumor progression involves modulation of tumor cell adhesion during migration and the degradation of ECM[3] during invasion. An intricate balance of proteases, their activators, and their inhibitors regulate both these processes during tumor invasion. ECM-degrading proteinases can be divided into three classes: (*a*) serine proteinases; (*b*) MMPs; and (*c*) cysteine proteinases. The urokinase plasminogen activator system is known to play a pivotal role in both tumor cell adhesion and matrix degradation. The serine protease uPA binds to its cell surface receptor uPAR and converts plasminogen to plasmin, a broad specificity serine protease with potent ECM-degrading properties. On its activation, plasmin degrades various ECM components, including fibrin, fibronectin, VN, laminin, and gelatins (1). In addition, plasmin can activate latent elastase and the MMPs, which are potent enzymes that can digest a variety of ECM components, including collagens, proteoglycans, elastin, laminin, and fibronectin.

Up-regulation of uPA (or its receptor) is associated with increased aggressiveness in diverse tumor types (2). In murine tumor models, expression or administration of uPAR antagonists has a marked inhibitory effect on the metastatic ability of cancers cells (3), primary tumor growth (4), and the down-regulation of uPAR, which leads to dormancy of carcinoma cells *in vivo* (5). In our earlier studies on human gliomas, expression of uPAR was greater in the high-grade tumors than in low-grade gliomas (6). The binding of uPA to uPAR is thought to play a major role in the invasion of glioblastoma cells into normal brain by concentrating the proteolytic activity at the leading edge of the tumor (6, 7). Stable transfection of a human glioblastoma cell line with antisense uPAR-expressing plasmid DNA has been shown to reduce the invasive properties of these cells both *in vitro* (8) and *in vivo* (9). Conversely, transfection of H4, a low-grade neuroglioma cell line which normally expresses low levels of uPAR, with full-length uPAR cDNA increased uPAR expression; the transfected cells showed a high invasive capability compared with the parental cells (10). Our studies on adenovirus-mediated delivery of the antisense uPAR gene showed suppression of glioma invasion and tumor growth (11). Taken together, these findings suggest that uPAR could be an important target for preventing cancer proliferation.

In addition, ligand binding of uPA to uPAR initiates interaction between a number of cell surface proteins, *e.g.*, VN, integrin receptors, and caveolin at focal adhesion sites (12). This process leads to intracellular phosphorylation of kinases, including cytokeratins, Src kinases, activation of the Jak/Stat pathway, and subsequently, kinases of the mitogen-activated protein kinase signaling pathways (13). There is evidence that uPA binding to uPAR-mediated signaling events results in the expression of cathepsin B and M_r 92,000 gelatinase (MMP-9) in monocytic cells (14). The ability of tumor cells to migrate into ECM *in vitro* is known to be mediated by the cooperative expression of a family of adhesion receptors called integrins and cell surface proteinases, such as uPA and MMPs (15). MMPs are proteolytic enzymes and their basic mechanism of action, the degradation of proteins, regulates various cell behaviors relevant to cancer biology. These include cancer cell growth, differentiation, apoptosis, migration, and invasion, as well as the regulation of tumor angiogenesis and immune surveillance. MMP-2 and MMP-9 are the two most abundant MMPs found in gliomas (16). We have shown previously that MMP-2, MMP-9, and MT-MMP are found in greater amounts during the progression of human gliomas and in glioma cell lines in culture (17–19). MMP-9 was also shown to be important in endothelial cell morphogenesis and the formation of capillaries in glial/endothelial cocultures *in vitro* (20). Furthermore, antisense oligonucleotides that blocked MMP-9 gene expression in SNB19 glioblastoma cells inhibited tumor formation in nude mice, thereby providing evidence that MMP-9 expression facilitates glioma invasion *in vivo* (21, 22).

Received 11/7/02; accepted 3/13/03.

The costs of publication of this article were defrayed in part by the payment of page charges. This article must therefore be hereby marked *advertisement* in accordance with 18 U.S.C. Section 1734 solely to indicate this fact.

[1] Supported by National Cancer Institute Grant CA 75557 (to J. S. R.).

[2] To whom requests for reprints should be addressed, at Division of Cancer Biology, Departments of Biomedical and Therapeutic Sciences and Neurosurgery, Box 1649, The University of Illinois College of Medicine at Peoria, Peoria, IL 61656. Phone: (309) 671-3445; Fax: (309) 671-3442.

[3] The abbreviations used are: ECM, extracellular matrix; uPA(R), urokinase-type plasminogen activator (receptor); MMP, matrix metalloproteinase; CMV, cytomegalovirus; MOI, multiplicity of infection; PFU, plaque-forming unit; VN, vitronectin; GFP, green fluorescent protein.

Gliomas are characterized by a high proliferation rate, extensive angiogenesis, and marked local invasion that makes these tumors resistant to the conventional treatment modalities of surgery, chemotherapy, and radiotherapy (23). There are great hopes that gene therapy can manage malignant tumors, including gliomas, and various approaches to gene therapy are being tested currently (24). On the basis of these previous observations, we hypothesized that manipulation of the expression of these two proteases in a single step may have a synergistic effect in inhibiting glioma tumor growth. In the present study, we constructed a replication-deficient recombinant adenovirus (Ad-uPAR-MMP-9) to efficiently deliver antisense uPAR and antisense MMP-9 genes to down-regulate uPAR and MMP-9 levels in human gliomas. We show that down-regulation of these two protease molecules has an additive effect in inhibiting glioma invasion and angiogenesis.

MATERIALS AND METHODS

Construction of Ad-uPAR-MMP-9. We have constructed previously an adenovirus expressing an antisense message for the uPAR gene using a pAd-uPAR vector containing the 300-bp DNA fragment of the 5′ end of the uPAR gene in the antisense orientation with a CMV promoter and bovine growth hormone polyadenylation signal (11). We then subcloned a 528-kb fragment of the 5′ end of the MMP-9 cDNA in an antisense orientation driven with its own independent promoter elements CMV and SV40 polyadenylation signal into pAd-uPAR. The sequence of the resulting clone pAd-uPAR-MMP-9 was confirmed, and the plasmid construct was cotransfected with 40–45-kb pJM17 vector into human embryonic kidney 293 cells to isolate recombinant Ads (25). Recombinant viral plaques were identified and amplified by PCR using primers specific for CMV and the SV40 polyadenylation signal. The virus particles were propagated in 293 cells and purified by ultracentrifugation in cesium chloride step gradients (25). The viral DNA was also sequenced to confirm the configuration of the expression cassette. A standard plaque assay was performed to determine the infectious particles. The control virus Ad-CMV has a CMV promoter and bovine growth hormone poly (A) signal but no gene insert in the E1-deleted region.

Cell Culture and Infection Conditions. We used the established human glioma cell line SNB19 for this study. The 293 human transformed embryonal kidney cell line was purchased from American Type Culture Collection (Manassas, VA). All cell lines were cultured at 37°C in media recommended by suppliers in a humidified atmosphere with 5% CO_2. Viral stocks were suitably diluted in serum-free medium to obtain the desired MOI or PFU and added to cell monolayers and tumor cell spheroids (1 ml/60-mm dish or 3 ml/100-mm dish), and the cells were then incubated at 37°C for 30 min. The necessary amount of culture medium with 10% FCS was added, and cells were incubated for the desired time periods.

Immunohistochemical Analysis. SNB19 cells (1×10^4) were seeded on VN-coated, eight-well chamber slides, incubated for 24 h, and infected with 100 MOI of Ad-CMV, Ad-uPAR, or Ad-uPAR-MMP-9. After another 72 h, cells were fixed with 3.7% formaldehyde and incubated with 1% BSA in PBS at room temperature for 1 h for blocking. After the slides were washed with PBS, either IgG anti-uPAR (rabbit) or IgG anti-MMP-9 (mouse) was added at a concentration of 1:500. The slides were incubated at room temperature for 1 h and washed three times with PBS to remove excess primary antibody. Cells were then incubated with antimouse Texas red conjugate or antirabbit FITC conjugate IgG (1:500 dilution) for 1 h at room temperature. The slides were then washed three times and covered with glass cover slips, and fluorescent photomicrographs were obtained.

Western Blot Analysis. Total cell lysates were prepared in extraction buffer containing 0.1 M Tris (pH 7.5), Triton X-114 (1.0%), EDTA (10 mM), aprotinin, and phenylmethylsulfonyl fluoride. Protein (20 μg) from these samples were separated under nonreducing conditions and transferred onto nylon membranes. The membranes were probed with rabbit antihuman uPAR polyclonal antibody (#399R; American Diagnostics, Inc., Greenwich, CT). Antirabbit horseradish peroxidase was used as the secondary antibody, and membranes were developed according to an enhanced chemiluminescence protocol (Amersham, Arlington Heights, IL).

Migration of Cells from Spheroids. Spheroids of SNB19 cells were prepared by suspending 2×10^6 SNB19 cells in DMEM, seeding cells onto 100-mm tissue culture plates coated with 0.75% agar, and culturing cells until spheroid aggregates formed. Spheroids measuring ~150 μm in diameter (~4×10^4 cells/spheroid) were selected and infected with adenovirus vectors (Ad-CMV, Ad-uPAR, or Ad-uPAR-MMP-9) at indicated MOI. Three days after infection, a single glioma spheroid was placed in the center of each well in VN-coated, 96-well microplates, and 200 μl of serum-free medium were added to each well. Spheroids were cultured at 37°C for 72 h, after which the spheroids were fixed and stained with Hema-3, and migration from the spheroids was assessed under light microscopy.

Zymography. SNB19 cells were infected with the indicated MOI of Ad CMV, Ad uPAR or Ad uPAR-MMP-9. The conditioned media and cell extracts were collected, and gelatin zymography was performed to detect MMP-9 levels as described previously (26).

Matrigel Invasion Assay. SNB19 cells were infected with 100 MOI of Ad-CMV, Ad-uPAR, or Ad-uPAR-MMP-9 for 4 days, and *in vitro* invasion of glioma cells was measured by the invasion of cells through Matrigel-coated (Collaborative Research, Inc., Boston, MA) transwell inserts (Costar, Cambridge, MA). Briefly, transwell inserts with an 8-μm pore size were coated with a final concentration of 0.7 mg/ml Matrigel, cells were trypsinized, and 200 μl of cell suspension (1×10^6 cells/ml) were added in triplicate wells. After a 24-h incubation period, cells that passed through the filter into the bottom wells were quantitated as described earlier (10, 11) and expressed as a percentage of the sum of cells in the top and bottom wells. Cells on the bottom side of the membrane were fixed, stained with Hema-3, and photographed.

Spheroid Invasion Assay. Multicellular glioma spheroids produced from SNB19 cells were cultured in 35-mm Petri dishes coated with 0.75% Noble agar prepared in DMEM. Briefly, 3×10^6 cells were suspended in 10 ml of medium, seeded onto 0.75% agar plates, and cultured until spheroids were formed. Spheroids of 100–200 μm in diameter were selected and infected with the indicated MOI of Ad-CMV and Ad-uPAR-MMP-9. After 3 days of infection, tumor spheroids were stained with the fluorescent dye 1′-dioctadecyl-3,3,3′,3′-tetramethylindocarbocyanineperchlorate and confronted with fetal rat brain aggregates that were stained with 3,3′-dioctadecyloxacarbocyanine perchlorate. Progressive destruction of fetal rat brain aggregates and invasion of SNB19 cells were observed by phase contrast microscopy and photographed as described previously (9).

***In Vitro* Angiogenic Assay.** SNB19 cells (2×10^4) were seeded in eight-well chamber slides and infected with the indicated MOIs of Ad-CMV, Ad-uPAR, and Ad-uPAR-MMP-9. After a 24-h incubation period, the medium was removed, and 4×10^4 human dermal endothelial cells were seeded and allowed to coculture for 72 h. Endothelial cells were stained for factor VIII antigen for 1 h after fixing the cells in 3.7% formaldehyde and blocking with 2% BSA. Factor VIII antibody was purchased from the DAKO Corp. (Carpinteria, CA). The cells were washed with PBS and incubated with FITC-conjugated secondary antibody for 1 h. The specimens were then washed and examined with confocal scanning laser microscopy (20).

Animal Experiments. For the intracranial tumor model, SNB19 cells that express GFP were infected in culture with 100 MOI of Ad-CMV or 50 MOI of Ad uPAR-MMP-9 for 5 days, trypsinized, counted, and injected intracranially into nude mice. At the end of the 4-week follow-up period (*e.g.*, when the control mice start showing symptoms), the mice were killed via cardiac perfusion with formaldehyde, the brains were removed, and frozen sections were prepared and observed for GFP fluorescence. The 3–5-μm sections were blindly reviewed and scored semiquantitatively for tumor size in each case. The average cross-sectional diameter was used to calculate tumor size and compared with the controls and treated group. The variation between the sections in each group was <10%. For the tumor regression experiments, U87-MG cells (5×10^6) were s.c. injected into nude mice, and tumor formation was followed for ≤4 weeks. After 8–10 days, when tumor size had reached 4–5 mm, the mice were injected with 5×10^8 PFUs of either Ad-CMV or Ad-uPAR-MMP-9 every other day for a total of five times. Tumor size was measured every 2nd day, and tumor volume was calculated with the formula $1/6\Pi\ (R_{max})^2 \times (R_{min})^2$, where R_{max} and R_{min} are the maximum and minimum tumor radii, respectively.

RESULTS

Ad-uPAR-MMP-9 Infection Decreased uPAR Protein Levels as Determined by Western Blotting. Western blot analysis was performed to examine the effect of the replication-deficient Ad-CMV, Ad-uPAR, and Ad-uPAR-MMP-9 infections on uPAR protein levels in SNB19 cells. Fig. 1*A* shows a dose-dependent decrease in uPAR protein levels. There was a significant decrease in cells infected with 25 MOI; cells infected with 50 MOI of Ad-uPAR-MMP-9 had a 90% reduction in uPAR protein levels. The decrease in uPAR protein was also related to time (Fig. 1*B*). SNB19 cells infected at 50 MOI showed a significant decrease by day 3, and the decrease reached 90% by day 4. A similar decrease in uPAR levels by the single gene construct Ad-uPAR from the standpoint of dose and time was seen at a much higher dose (100 MOI) and later time interval (day 6).

Ad-uPAR-MMP-9 Infection Decreased MMP-9 Levels in SNB19 Cells. Gelatin zymography was performed to examine the effect of Ad-uPAR-MMP-9 infection on MMP-9 enzymatic activity in SNB19 cells. Fig. 1*C* shows that the MMP-9 enzymatic activity (M_R 92,000) decreased in a dose-dependent fashion with increasing MOI. Densitometric quantification of MMP-9 enzymatic activity showed a significant decrease in the cells infected with Ad-uPAR-MMP-9 at 50 MOI. This decrease reached >90% of the cells infected with Ad-uPAR-MMP-9 at 100 MOI (with the percentage decrease determined relative to those in Ad-CMV-infected control cells). The decrease in MMP-9 enzymatic activity was also related to time, because SNB19 cells infected with 50 MOI of Ad-uPAR-MMP-9 showed a 90% decrease in MMP-9 activity by day 5 (Fig. 1*D*).

Ad-uPAR-MMP-9 Infection Decreased uPAR and MMP-9 Immunoreactivity and Angiogenesis. Immunohistochemical analyses of SNB19 cells infected with Ad-uPAR-MMP-9 showed intense staining of uPAR and MMP-9 in mock-infected cells and was comparable with that of the Ad-CMV-infected cells (Fig. 2*A*). Very weak signals were detected in Ad-uPAR-MMP-9-infected cells, and Ad-uPAR-infected cells showed intermediate staining when compared with mock- or Ad-CMV-infected cells (Fig. 2*A*). A tube formation assay was used to determine the capability of the bicistronic virus to regulate angiogenesis in tumors. In the presence of SNB19 cell, the endothelial cells formed capillary-like structures within 18 h. As seen in Fig. 2*B*, 100 MOI of Ad-uPAR could repress capillary formation by ~50% when compared with mock- or Ad-CMV-infected cocultures. Endothelial cells cocultured with only 10 MOI of Ad-uPAR-MMP-9 could inhibit capillary formation by ~80%. Increasing the MOI of the bicistronic vector progressively inhibited capillary-like structures in a dose-dependent manner.

Ad-uPAR-MMP-9 Infection Decreased Migration of Glioma Cells from Spheroids. The control spheroids showed significant cell migration and were comparable with the spheroids infected with Ad-CMV (Fig. 3*A*). The spheroids infected with 100 MOI of Ad-uPAR showed significant reduction in cell migration. Spheroids infected with 10 MOI of Ad-uPAR-MMP-9 showed significantly less migration compared with that of the control and Ad-uPAR-infected spheroids. SNB19 spheroids infected with 25 and 50 MOI of Ad-uPAR-MMP-9 did not attach to the VN-coated chamber slides in all four replicates, and, no cell migration was detected.

Ad-uPAR-MMP-9 Infection Decreased Invasiveness of SNB19 Cells. We used two models (Matrigel invasion and spheroid) to study the effect of the Ad-uPAR-MMP-9 bicistronic vector on glioma invasion. Cells infected with Ad-CMV, Ad-uPAR, and Ad-uPAR-MMP-9 were allowed to invade through Matrigel for 24 h. The staining of Ad-uPAR- or Ad-uPAR-MMP-9-transfected cells that invaded through the Matrigel was significantly less compared with mock- and Ad-CMV-infected cells (Fig. 3*B*). Only 25% of Ad-uPAR-infected cells invaded compared with the Ad-CMV-infected cells. In the Ad-uPAR-MMP-9-infected cells, a 10-fold decrease in the invasive potential of the glioma cells was seen when compared with the Ad-CMV-infected cells (Fig. 3*C*).

To study the invasion of SNB19 cells in a more three-dimensional system, tumor spheroids and fetal rat brain aggregates stained with the fluorescent dyes 1′-dioctadecyl-3,3,3′,3′-tetramethylindocarbocyanineperchlorate or 3,3′-dioctadecyloxacarbocyanine perchlorate were cocultured. Staining of the cells with these dyes allows better visualization and characterization of the invasive pattern via confocal laser scanning microscopy than other *in vitro* invasion assays. Spheroids of multicellular SNB19 cells infected with mock, 25, 50, or 100 MOI of Ad-uPAR-MMP-9 were confronted with fetal rat brain aggregates, and images were obtained using confocal microscopy. In the Ad-

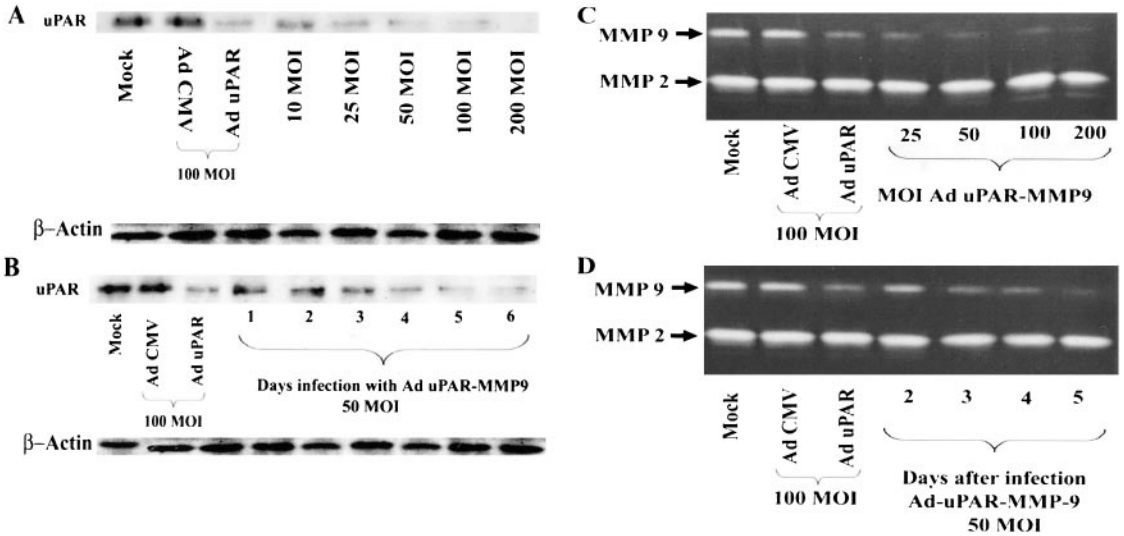

Fig. 1. Western blot analysis for uPAR and gelatin zymography for MMP-9. SNB19 cells infected with Ad-CMV, Ad-uPAR, and Ad-uPAR-MMP-9 for 4 days at the indicated MOI and uPAR levels were determined by Western blotting (*A*). SNB19 cells infected with Ad-CMV, Ad-uPAR, and Ad-uPAR-MMP-9 at 100 MOI at the indicated time points and uPAR protein levels were determined by Western blotting (*B*). MMP-9 activity of SNB19 cells infected with Ad-CMV, Ad-uPAR, and Ad-uPAR-uPA for 4 days in serum-free medium at the indicated MOI as determined by gelatin zymography (*C*). MMP-9 activity of SNB19 cells infected with Ad-CMV, Ad-uPAR, and Ad-uPAR-MMP-9 at 100 MOI at the indicated time points as determined by gelatin zymography (*D*).

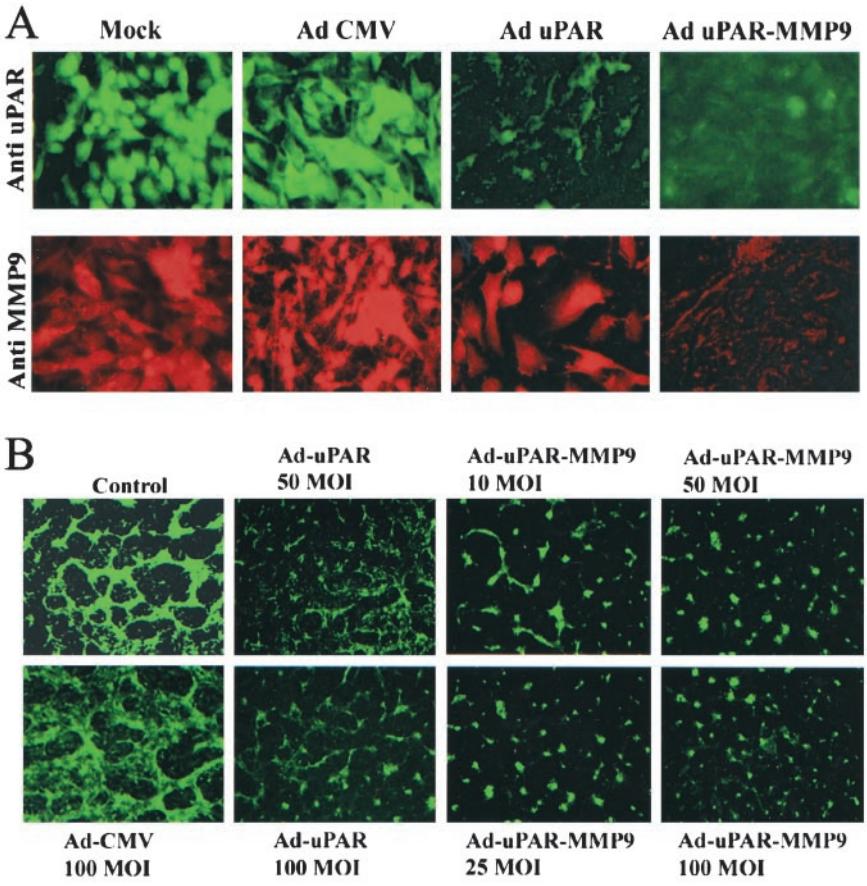

Fig. 2. In *A*, Ad-uPAR-MMP-9 infection decreased uPAR and MMP-9 levels as shown by immunohistochemical analysis. SNB19 cells (1×10^4) were seeded in eight-well chamber slides, incubated for 24 h, and infected with 100 MOI of Ad-CMV, Ad-uPAR, or Ad-uPAR-MMP-9. After 72 h, cells were fixed, washed for 1 h with blocking buffer, and stained for uPAR and MMP-9 using specific antibodies for either uPAR or MMP-9. In *B*, Ad-uPAR-MMP-9 inhibited tumor-induced angiogenesis. SNB19 cells (2×10^4) were seeded in eight-well chamber slides and infected with indicated MOI of Ad-CMV, Ad-uPAR, and Ad-uPAR-MMP-9. After 24-h incubation, the medium was removed, and the cells were cocultured with 4×10^4 human endothelial cells. After 72 h, endothelial cells were stained for factor VIII antigen and examined under a confocal scanning laser microscope.

CMV-infected spheroids, complete invasion of the fetal rat brain aggregate was observed after 72 h. In the case of spheroids infected with 25 MOI of the bicistronic adenovirus, only a small region of cell colocalization was seen, and no significant invasion was noticed at 72 h. In the case of spheroids infected with 50 MOI of the same virus, colocalization was seen but significantly less than that seen in the 25 MOI-infected spheroids. In the case of the spheroids infected with 100 MOI of the virus, no visible colocalization was seen, and the glioma cell spheroids completely failed to invade the rat brain aggregates (Fig. 4*A*). Glioma spheroids infected with Ad-CMV progressively invaded by ~90% at 72 h. However, glioma spheroids infected with Ad-uPAR-MMP-9 at 25, 50, and 100 MOI in cocultures with fetal rat brain aggregates invaded only 2–15% at 72 h. (Fig. 4*B*).

Ad-uPAR-MMP-9 Inhibits Tumor Growth in Mice. SNB19 variants that express GFP were infected with mock, Ad-CMV, or Ad-uPAR-MMP-9 (50 MOI) and then injected intracerebrally into nude mice. All 10 of the mice in each group injected with mock- and Ad-CMV-infected cells developed tumors, whereas none of the animals injected with Ad-uPAR-MMP-9-infected cells developed any significant tumors over a 4–5 week follow-up period (Fig. 4*C*). Quantitation of tumor size showed a significant reduction ($P < 0.001$) in Ad-uPAR-MMP-9-infected cells compared with mock and Ad-CMV-infected cells (Fig. 4*D*). In a separate experiment, the *in vivo* intratumoral effect of Ad-uPAR-MMP-9 injection was analyzed in nude mice bearing U-87 s.c. tumors. When tumor size reached ~5–6 mm in diameter, 10 mice in each group received three intratumoral injections of either Ad-CMV or Ad-uPAR-MMP-9 at 5×10^8 PFU every 48 h. Tumor growth was recorded from the first injection (day 0). All 10 mice injected with the Ad-uPAR-MMP-9 vector showed tumor regression beginning on day 5 after the third injection, and regression continued for 20 days, at which ~80% of inhibition was observed in the treated group (Fig. 5*A*). More than 90–95% inhibition of tumor growth in the Ad-uPAR-MMP-9-treated group was observed compared with the Ad-CMV-injected tumors (Fig. 5*A*). Fig. 5*B* shows that Ad-uPAR-MMP-9-treated animals showed reduced tumor size compared with Ad-CMV-treated animals.

DISCUSSION

The study of glioma invasion includes various aspects, such as glioma cell genotype, its ability to secrete proteases, which can break down extracellular barriers thereby facilitating motility, the relationship between the tumor cells and surrounding stroma, and finally, the mechanics of the cytoskeleton that lead to the highly invasive phenotype. As gene therapy technology improves, there are an increasing number of therapeutic agents that permit manipulation of cancerous cells. Targeting specific molecules unique to tumor cells by antisense inhibition was shown to have potential effectiveness in cancer therapy. Because many clinical studies are already based on protease activity inhibition and it is known that serine proteinases, such as uPA, and metalloproteinases, such as MMPs, are essential for cell invasion, we simultaneously targeted the uPA receptor and a metalloprotease (uPAR and MMP-9) by using an antisense gene delivery strategy with a replication-deficient recombinant Ad vector. The anticancer effect of Ad-uPAR-MMP-9 was demonstrated in *in vitro* and *in vivo* studies using the SNB19 and U87 MG glioma cell lines. We demonstrated that adenoviral delivery of antisense uPAR and MMP-9 genes has an additive effect in tumor regression as compared with our previous studies on the expression of the single Ad-mediated antisense uPAR and antisense MMP-9 constructs in SNB19 cells.

Ad-uPAR-MMP-9 infection significantly reduced uPAR and MMP-9 levels in SNB19 cells as determined by immunohistochemi-

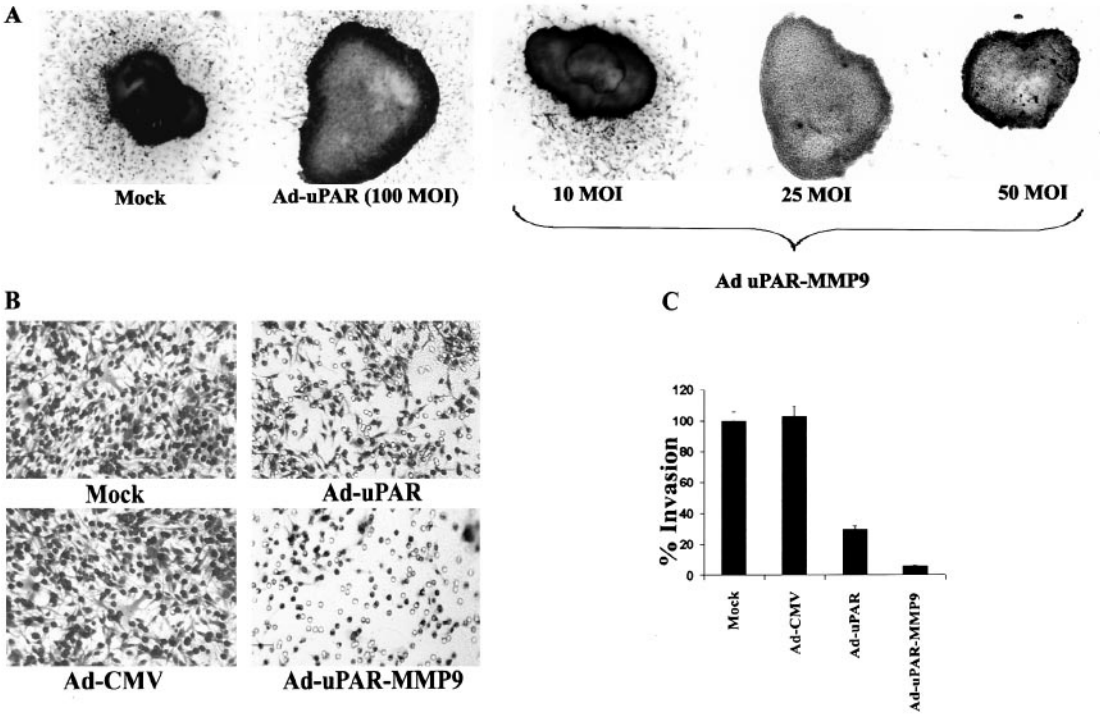

Fig. 3. *A*, migration of SNB19 cells infected with Ad-uPAR-MMP-9. SNB19 cells (3×10^6 cells) were suspended in DMEM, seeded onto 0.5% agar-coated plates, and cultured until spheroids were formed. Spheroids of 100–200 μm in diameter were selected and infected with mock, 10 MOI, 25 MOI, and 50 MOI of Ad-uPAR-MMP-9 (another set of spheroids was trypsinized to determine their cell number). After 3 days, single glioma spheroids were placed in the center of a VN-coated well in a 96-well plate and cultured at 37°C for 48 h. At the end of the migration assay, spheroids were fixed and stained with Hema-3 and photographed. In *B*, Ad-uPAR-MMP-9 infection inhibits invasion of SNB19 cells. SNB19 cells were infected with 100 MOI of either Ad-CMV or Ad-uPAR-MMP-9. Four days later, 1×10^6 cells were allowed to invade for 24 h through transwell inserts (8-μm pores) coated with Matrigel. The cells that invaded through the Matrigel-coated inserts were stained, counted, and photographed under a light microscope at $\times$20 magnification (*C*), and invasion was quantified as described in "Materials and Methods." Data shown are the average values from four separate experiments from each group ($\pm$SD; $P < 0.001$).

cal analysis and Western blotting. uPAR and MMP-9 protein expression decreased in a dose-dependent fashion with a >90% decrease in cells infected at 50 MOI. This decrease was more significant when compared with the Ad-uPAR infection where a less similar decrease in the protein levels was observed when the cells were infected with 100 MOI of Ad-uPAR. A similar decrease in MMP-9 enzyme activity was observed as determined by gelatin zymography. We then determined the invasive potential of SNB19 cells after infection with Ad-uPAR-MMP-9 and compared it with the vector controls and Ad-uPAR infection in Matrigel and spheroid assays. Ad-uPAR-MMP-9 infection had a more superior effect in inhibiting glioma invasion in both the model systems compared with Ad-uPAR infection. Several reports have demonstrated the role of uPAR and MMP-9 in ECM degradation, which is a key step for cancer invasion. uPAR levels correlated strongly with metastatic potential in human cancer cell lines of melanoma, breast, lung, and colon (26–28). Previous studies have shown that the uPAR antibody reduces tumor cell invasion in colon cancers and glioblastomas (29, 30). Our previous work with stably transfected antisense uPAR SNB19 glioma cells failed to form tumors in nude mice (9), and the adenovirus-mediated delivery of antisense uPAR gene suppressed glioma invasion and growth (11). Similarly, reducing uPAR levels by using antisense oligonucleotides was also found to inhibit tumor growth, invasion, and metastasis in some cancers (3, 31). However, other studies on colon cancer metastasis have shown that antisense uPAR mRNA could only partially control metastasis. This may be attributable to several factors in the uPA system, including uPAR binding capacity, the amount of uPA available for binding, presence of the endogenous uPA inhibitor PAI-1, as well as the ratio of potent active uPA and inactive ligands occupied on uPAR. All these factors are involved in determining the capacity of tumor invasion and metastasis. In addition, other proteases, including matrix metalloproteases, may compensate for the lack of uPA activity and uPAR protein. Therefore, apart from the reduction of uPAR expression, we simultaneously targeted MMP-9 to obtain maximum inhibition of glioma invasion.

We also assessed the effect of the bicistronic construct in migration because it is one of the first steps in invasion. Our results show that SNB19 spheroids infected with Ad-uPAR-MMP-9 have significantly reduced migration as compared with parental and vector controls, as well as more distinct inhibition than the Ad-uPAR-infected SNB19 spheroids. In addition to regulating plasminogen activation at the cell surface, recent studies indicate that uPAR possesses other cellular activities, including an ability to generate intracellular signal transduction, regulate integrin function, and directly bind VN (12). It has also been shown that disruption of the caveolin-integrin-uPAR complex inactivates signaling through extracellular signal-regulated kinase and adhesion and migration in kidney epithelial and smooth muscle cells (12). Studies on leukocyte migration to the sites of inflammation using $uPAR^{-/-}$ demonstrated that an intact uPAR molecule, probably by activating β2 integrins, is required for *in vivo* transendothelial migration (32). In the present study, SNB19 spheroids infected with Ad-uPAR-MMP-9 failed to adhere to the VN-coated plates at 50 MOI. Recent studies document that MMP-9 is involved in several steps of cancer development including tumor cell migration. The localization of MMP-9 to specialized surface protrusions called invadopodia on the cell membrane by binding to CD44, a receptor for hyaluronan, is required to promote tumor cell migration (31). MMP-9 is also produced by epithelial cells and actively involved in the migration of repairing bronchial epithelial cells (33). Using inhibitory monoclonal antibodies and unselective MMP inhibitors, it was found that gelatinase B is crucial for the migration of Langerhans and dermal dendrite cells from human and murine skin (34).

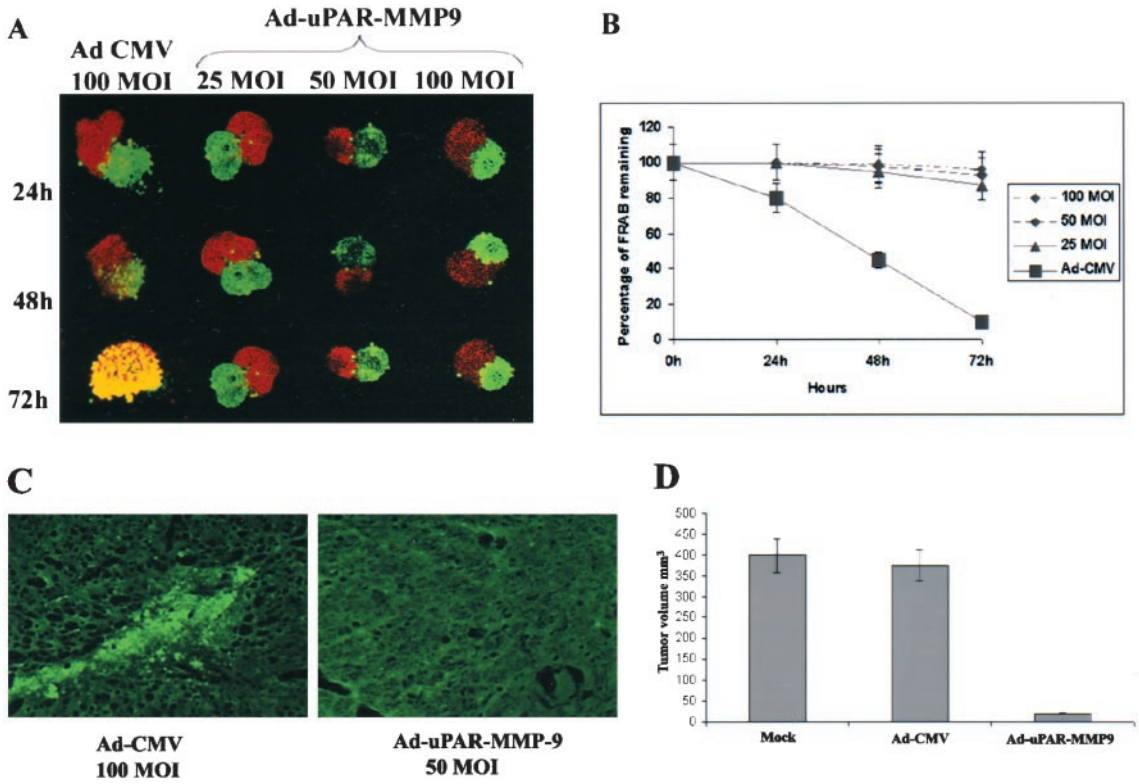

Fig. 4. A, Ad-uPAR-MMP-9 infection inhibits SNB19 spheroid invasiveness into rat brain aggregates. Tumor spheroids (red fluorescence) 100–200 μm in diameter were infected with 100 MOI of Ad-CMV and 25, 50, and 100 MOI of Ad-uPAR-MMP-9 and cocultured with fetal rat brain aggregates. After 3 days, progressive destruction of fetal rat brain aggregates (green fluorescence) was observed using confocal laser scanning microscopy. *B,* quantification of remaining fetal rat brain aggregates by SNB19 spheroids infected with Ad-CMV or Ad-uPAR-MMP-9 vectors as described in "Materials and Methods." Data shown are the mean ± SD values from four separate experiments for each group ($*P < 0.001$). In *C,* Ad-uPAR-MMP-9 infection inhibits intracerebral tumor formation. SNB19 glioblastoma cells were infected with PBS (*Mock*) or 100 MOI of Ad-CMV or 50 MOI of Ad-uPAR-MMP-9 for 4 days, trypsinized, counted, and then inoculated intracerebrally (1×10^6 cells in 10 μl of PBS) into nude mice (10 mice in each group). The animals were examined for tumor formation over a 5–6 week period, and tumor sizes were estimated from tumor sections of GFP-expressing cells. In *D,* semiquantitation of tumor volume in mock/Ad-CMV and Ad-uPAR-MMP-9 infected SNB19 cells 4 weeks after intracranial injection of these cells as described in "Materials and Methods." In *D,* data shown are the mean ± SD values from 10 animals from each group ($*P < 0.001$).

We then tested the effect of the bicistronic construct on tumor growth. SNB19 cells infected with Ad-uPAR-MMP-9 (50 MOI) did not form any detectable tumors in nude mice. We have reported previously that apoptosis measured by DNA fragmentation was higher in the brains of animals injected with the antisense stable transfectants of antisense uPAR than in those injected with the parental cells (35). Alternatively, Ad-uPAR-MMP-9 was injected directly into pre-established U87 s.c. tumors. Despite low doses (5×10^8 PFU $\times$ 3) compared with our previous work with Ad-uPAR (5×10^9 PFU $\times$ 5; Ref. 11), there was significant tumor regression for ≤12 weeks. This effect could be a result of simultaneously targeting uPAR and MMP-9, which have many biological roles, including cell adhesion and migration, resulting in decreased invasion/angiogenesis, which in turn could lead to tumor growth suppression.

To understand the underlying mechanism of tumor growth inhibition, we analyzed the effect of this bicistronic construct on angiogenesis. The importance of the interaction between uPA and uPAR during angiogenesis has also been demonstrated in a number of *in vivo* systems. Adenovirally delivered NH_2-terminal fragments specifically inhibited tumor angiogenesis in syngeneic and xenograft murine tu-

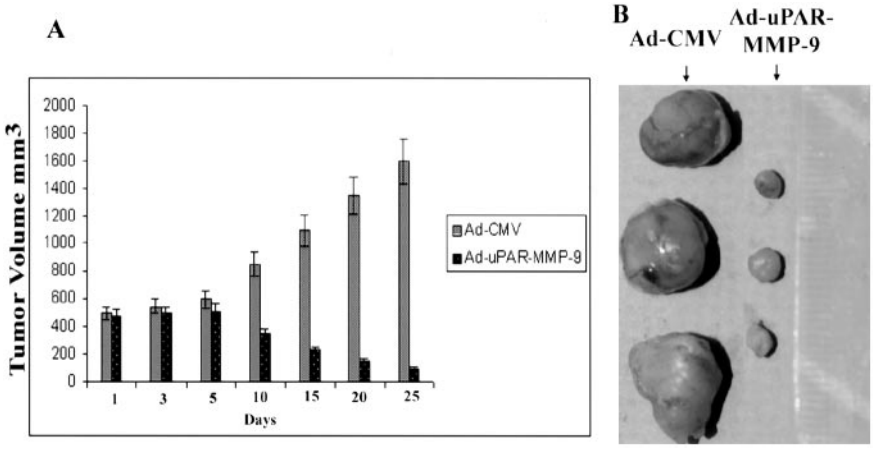

Fig. 5. Growth inhibition of pre-established tumors. In *A,* U87 cells (5×10^6) in 100 μl of PBS were injected s.c. into nude mice. After 8–10 days, the resultant 5–6-mm s.c. tumors were injected intratumorally with 5×10^8 PFU of either Ad-CMV (vector control) or Ad-uPAR-MMP-9 in 25-μl volumes. A total of three injections was given, one every other day, and the tumor size was measured with calipers. Tumor volumes are shown as mean ± SD ($*P < 0.001$). In *B,* tumors from these animals were dissected 20 days after the third injection with Ad-CMV and Ad-uPAR-MMP-9.

mor models (36). Similarly, a fusion protein consisting of the receptor-binding, NH_2-terminal fragment of uPA and Fc portion of human IgG, which functions as a high-affinity uPAR antagonist, inhibited basic fibroblast growth factor-induced angiogenesis in s.c. injected Matrigel (4). Microvessel density was markedly decreased in a homologous immunocompetent model of tumor cells transfected with a mutant murine uPA that retains receptor binding but not proteolytic activity (37). An octamer peptide derived from the nonreceptor binding region of uPA was shown to inhibit tumor growth and angiogenesis in breast cancer (38) and in combination with cisplatin in glioblastomas (39). In the present study, although Ad-uPAR (100 MOI) infection inhibited capillary-like network formation when SNB19 cells were cocultured with human dermal endothelial cells, Ad-uPAR-MMP-9 was very effective in inhibiting capillary formation even at very low concentrations (10 MOI). With respect to MMPs, potential targets for inhibiting angiogenesis include the gelatinases and MT-MMPs. MMP-9 has been shown to be important for angiogenesis in two transgenic models of tumor progression, the K14-HPV16 skin cancer model (40) and the RIP1-Tag2 insulinoma model (41). Genetic studies with MMP-9 knockout mice showed impaired angiogenesis during development, thereby supporting the role of MMP-9 in angiogenesis (42).

Extracellular proteases have been shown to cooperatively influence matrix degradation and tumor cell invasion through proteolytic cascades, with individual proteases having distinct roles in tumor growth, invasion, migration, and angiogenesis. This proteolytic cascade process releases various growth and differentiation factors that are sequestered on the cell surface or within the ECM, which contribute to the evolution of a migratory or invasive cell phenotype (43). Results accumulated over the last decade suggest that uPAR is also involved in motility control through other mechanisms. These include induction of signal transduction events after ligation with uPA, binding to the ECM molecule VN, and association with integrins and other transmembrane partners (44). Binding of uPAR to integrins may enrich integrin clusters with signaling molecules, such as Src-family kinases that localize to rafts and are important to integrin function. Signals derived from integrin/uPAR complexes promote the function of other integrins, regulating cell matrix interactions (45). Integrins have also been found to cooperate with metalloproteases to promote tumor cell invasion and angiogenesis (46). Lund *et al.* (47) demonstrated the requirement for both plasminogen deficiency and metalloprotease inhibition for complete inhibition of the healing process, indicating that there is a functional overlap between the two classes of matrix-degrading proteases. These findings suggest that effective arrest of cancer progression will require the combined use of inhibitors of MMPs and inhibitors of the plasmin/Plg activation system.

In the clinical setting, tumors exhibit a diverse array of mutated signaling pathways. In light of our understanding of the complex nature of uPAR and MMP-9 in multiple biological events, such as migration, adhesion, angiogenesis, tumorigenicity, and differentiation, our attempt to simultaneously target both uPAR and MMP-9 has clear clinical implications with a broad field of action. Although recombinant adenoviruses are excellent gene delivery vehicles for cancer gene therapy, toxicity caused by high vector doses and therapeutic effectiveness of Ad-mediated gene transfer could be limiting factors. It has been reported recently that preimmunity can inhibit systemic expression from adenoviral vectors, but at high vector doses, it may potentiate hepatotoxicity (48). Our present work addresses the toxicity issue to some extent, because our results clearly demonstrate that the bicistronic construct (Ad-uPAR-MMP-9) had a more prominent effect in inhibiting tumor invasion and growth at much lower doses compared with a single gene construct (Ad-uPAR). Consequently, these findings emphasize the potential of this protocol, although adenoviral delivery of genes is known to be transient and to last for only 4–6 weeks. Nonetheless, the use of novel vectors with long-term expression of genes at therapeutic levels or with modified fibers to specifically infect gliomas is necessary to treat intracranial tumors.

REFERENCES

1. Mignatti, P., and Rifkin, D. B. Biology and biochemistry of proteinases in tumor invasion. Physiol. Rev., *73:* 161–195, 1993.
2. Blasi, F. Proteolysis, cell adhesion, chemotaxis, and invasiveness are regulated by the u-PA-u-PAR-PAI-1 system. Thromb. Haemost., *82:* 298–304, 1999.
3. Crowley, C. W., Cohen, R. L., Lucas, B. K., Liu, G., Shuman, M. A., and Levinson, A. D. Prevention of metastasis by inhibition of the urokinase receptor. Proc. Natl. Acad. Sci. USA, *90:* 5021–5025, 1993.
4. Min, H. Y., Doyle, L. V., Vitt, C. R., Zandonella, C. L., Stratton-Thomas, J. R., Shuman, M. A., and Rosenberg, S. Urokinase receptor antagonists inhibit angiogenesis and primary tumor growth in syngeneic mice. Cancer Res., *56:* 2428–2433, 1996.
5. Yu, W., Kim, J., and Ossowski, L. Reduction in surface urokinase receptor forces malignant cells into a protracted state of dormancy. J. Cell Biol., *137:* 767–777, 1997.
6. Yamamoto, M., Sawaya, R., Mohanam, S., Rao, V. H., Bruner, J. M., Nicolson, G. L., and Rao, J. S. Expression and localization of urokinase-type plasminogen activator receptor in human gliomas. Cancer Res., *54:* 5016–5020, 1994.
7. Gladson, C. L., Pijuan-Thompson, V., Olman, M. A., Gillespie, G. Y., and Yacoub, I. Z. Up-regulation of urokinase and urokinase receptor genes in malignant astrocytoma. Am. J. Pathol., *146:* 1150–1160, 1995.
8. Mohanam, S., Chintala, S. K., Go, Y., Bhattacharya, A., Venkaiah, B., Boyd, D., Gokaslan, Z. L., Sawaya, R., and Rao, J. S. In vitro inhibition of human glioblastoma cell line invasiveness by antisense uPA receptor. Oncogene, *14:* 1351–1359, 1997.
9. Go, Y., Chintala, S. K., Mohanam, S., Gokaslan, Z., Venkaiah, B., Bjerkvig, R., Oka, K., Nicolson, G. L., Sawaya, R., and Rao, J. S. Inhibition of in vivo tumorigenicity and invasiveness of a human glioblastoma cell line transfected with antisense uPAR vectors. Clin. Exp. Metastasis, *15:* 440–446, 1997.
10. Mohanam, S., Chintala, S. K., Mohan, P. M., Sawaya, R., Lagos, G. K., Gokaslan, Z. L., Kouraklis, G. P., and Rao, J. S. Increased invasion of neuroglioma cells transfected with urokinase plasminogen activator receptor cDNA. Int. J. Oncol., *13:* 1285–1290, 1998.
11. Mohan, P. M., Chintala, S. K., Mohanam, S., Gladson, C. L., Kim, E. S., Gokaslan, Z. L., Lakka, S. S., Roth, J. A., Fang, B., Sawaya, R., Kyritsis, A. P., and Rao, J. S. Adenovirus-mediated delivery of antisense gene to urokinase-type plasminogen activator receptor suppresses glioma invasion and tumor growth. Cancer Res., *59:* 3369–3373, 1999.
12. Chapman, H. A., Wei, Y., Simon, D. I., and Waltz, D. A. Role of urokinase receptor and caveolin in regulation of integrin signaling. Thromb. Haemost., *82:* 291–297, 1999.
13. Irigoyen, J. P., Munoz-Canoves, P., Montero, L., Koziczak, M., and Nagamine, Y. The plasminogen activator system: biology and regulation. Cell Mol. Life Sci., *56:* 104–132, 1999.
14. Rao, N. K., Shi, G. P., and Chapman, H. A. Urokinase receptor is a multifunctional protein: influence of receptor occupancy on macrophage gene expression. J. Clin. Investig., *96:* 465–474, 1995.
15. Ruoslahti, E. Integrins. J. Clin. Investig., *87:* 1–5, 1991.
16. Forsyth, P. A., Wong, H., Laing, T. D., Rewcastle, N. B., Morris, D. G., Muzik, H., Leco, K. J., Johnston, R. N., Brasher, P. M., Sutherland, G., and Edwards, D. R. Gelatinase-A (MMP-2), gelatinase-B (MMP-9) and membrane type matrix metalloproteinase-1 (MT1-MMP) are involved in different aspects of the pathophysiology of malignant gliomas. Br. J. Cancer, *79:* 1828–1835, 1999.
17. Rao, J. S., Steck, P. A., Mohanam, S., Stetler-Stevenson, W. G., Liotta, L. A., and Sawaya, R. Elevated levels of M(r) 92, 000 type IV collagenase in human brain tumors. Cancer Res, *53:* 2208–2211, 1993.
18. Sawaya, R., Go, Y., Kyritisis, A. P., Uhm, J., Venkaiah, B., Mohanam, S., Gokaslan, Z. L., and Rao, J. S. Elevated levels of Mr 92, 000 type IV collagenase during tumor growth in vivo. Biochem. Biophys. Res. Commun., *251:* 632–636, 1998.
19. Chintala, S. K., Tonn, J. C., and Rao, J. S. Matrix metalloproteinases and their biological function in human gliomas. Int. J. Dev. Neurosci., *17:* 495–502, 1999.
20. Chandrasekar, N., Jasti, S., Alfred-Yung, W. K., Ali-Osman, F., Dinh, D. H., Olivero, W. C., Gujrati, M., Kyritsis, A. P., Nicolson, G. L., Rao, J. S., and Mohanam, S. Modulation of endothelial cell morphogenesis in vitro by MMP-9 during glial-endothelial cell interactions. Clin. Exp. Metastasis, *18:* 337–342, 2000.
21. Kondraganti, S., Mohanam, S., Chintala, S. K., Kin, Y., Jasti, S. L., Nirmala, C., Lakka, S. S., Adachi, Y., Kyritsis, A. P., Ali-Osman, F., Sawaya, R., Fuller, G. N., and Rao, J. S. Selective suppression of matrix metalloproteinase-9 in human glioblastoma cells by antisense gene transfer impairs glioblastoma cell invasion. Cancer Res., *60:* 6851–6855, 2000.
22. Lakka, S. S., Jasti, S. L., Gondi, C., Boyd, D., Chandrasekar, N., Dinh, D. H., Olivero, W. C., Gujrati, M., and Rao, J. S. Downregulation of MMP-9 in ERK-mutated stable transfectants inhibits glioma invasion in vitro. Oncogene, *21:* 5601–5608, 2002.
23. Giese, A., and Westphal, M. Glioma invasion in the central nervous system. Neurosurgery, *39:* 235–250, 1996.
24. Anderson, W. F. Excitement in gene therapy! Hum. Gene Ther., *12:* 1483–1484, 2001.
25. Graham, F. L., and Prevec, L. Manipulation of adenovirus vectors. *In:* E. J. Murray (ed.), Methods in Molecular Biology, pp. 109–127. Clifton, NJ: The Humana Press, 1991.

26. Hollas, W., Soravia, E., Mazar, A., Henkin, J., Blasi, F., and Boyd, D. Decreased urokinase receptor expression by overexpression of the plasminogen activator in a colon cancer cell line. Biochem. J., *285:* 629–634, 1992.
27. Pedersen, H., Brunner, N., Francis, D., Osterlind, K., Ronne, E., Hansen, H. H., Dano, K., and Grondahl-Hansen, J. Prognostic impact of urokinase, urokinase receptor, and type 1 plasminogen activator inhibitor in squamous and large cell lung cancer tissue. Cancer Res., *54:* 4671–4675, 1994.
28. Stahl, A., and Mueller, B. M. Binding of urokinase to its receptor promotes migration and invasion of human melanoma cells *in vitro*. Cancer Res., *54:* 3066–3071, 1994.
29. Reiter, L. S., Kruithof, E. K., Cajot, J. F., and Sordat, B. The role of the urokinase receptor in extracellular matrix degradation by HT29 human colon carcinoma cells. Int. J. Cancer, *53:* 444–450, 1993.
30. Mohanam, S., Sawaya, R., McCutcheon, I., Ali-Osman, F., Boyd, D., and Rao, J. S. Modulation of *in vitro* invasion of human glioblastoma cells by urokinase-type plasminogen activator receptor antibody. Cancer Res., *53:* 4143–4147, 1993.
31. Bourguignon, L. Y., Gunja-Smith, Z., Iida, N., Zhu, H. B., Young, L. J., Muller, W. J., and Cardiff, R. D. CD44v(3, 8–10) is involved in cytoskeleton-mediated tumor cell migration and matrix metalloproteinase (MMP-9) association in metastatic breast cancer cells. J. Cell. Physiol., *176:* 206–215, 1998.
32. Waltz, D. A., Fujita, R. M., Yang, X., Natkin, L., Zhuo, S., Gerard, C. J., Rosenberg, S., and Chapman, H. A. Nonproteolytic role for the urokinase receptor in cellular migration in vivo. Am. J. Respir. Cell Mol. Biol., *22:* 316–322, 2000.
33. Legrand, C., Gilles, C., Zahm, J. M., Polette, M., Buisson, A. C., Kaplan, H., Birembaut, P., and Tournier, J. M. Airway epithelial cell migration dynamics. MMP-9 role in cell-extracellular matrix remodeling. J. Cell Biol., *146:* 517–529, 1999.
34. Ratzinger, G., Stoitzner, P., Ebner, S., Lutz, M. B., Layton, G. T., Rainer, C., Senior, R. M., Shipley, J. M., Fritsch, P., Schuler, G., and Romani, N. Matrix metalloproteinases 9 and 2 are necessary for the migration of Langerhans cells and dermal dendritic cells from human and murine skin. J. Immunol., *168:* 4361–4371, 2002.
35. Kin, Y., Chintala, S. K., Go, Y., Sawaya, R., Mohanam, S., Kyritsis, A. P., and Rao, J. S. A novel role for the urokinase-type plasminogen activator receptor in apoptosis of malignant gliomas. Int. J. Oncol., *17:* 61–65, 2000.
36. Li, H., Lu, H., Griscelli, F., Opolon, P., Sun, L. Q., Ragot, T., Legrand, Y., Belin, D., Soria, J., Soria, C., Perricaudet, M., and Yeh, P. Adenovirus-mediated delivery of a uPA/uPAR antagonist suppresses angiogenesis-dependent tumor growth and dissemination in mice. Gene Ther., *5:* 1105–1113, 1998.
37. Evans, C. P., Elfman, F., Parangi, S., Conn, M., Cunha, G., and Shuman, M. A. Inhibition of prostate cancer neovascularization and growth by urokinase-plasminogen activator receptor blockade. Cancer Res., *57:* 3594–3599, 1997.
38. Guo, Y., Higazi, A. A., Arakelian, A., Sachais, B. S., Cines, D., Goldfarb, R. H., Jones, T. R., Kwaan, H., Mazar, A. P., and Rabbani, S. A. A peptide derived from the nonreceptor binding region of urokinase plasminogen activator (uPA) inhibits tumor progression and angiogenesis and induces tumor cell death in vivo. FASEB J., *14:* 1400–1410, 2000.
39. Mishima, K., Mazar, A. P., Gown, A., Skelly, M., Ji, X. D., Wang, X. D., Jones, T. R., Cavenee, W. K., and Huang, H. J. A peptide derived from the non-receptor-binding region of urokinase plasminogen activator inhibits glioblastoma growth and angiogenesis in vivo in combination with cisplatin. Proc. Natl. Acad. Sci. USA, *97:* 8484–8489, 2000.
40. Coussens, L. M., Tinkle, C. L., Hanahan, D., and Werb, Z. MMP-9 supplied by bone marrow-derived cells contributes to skin carcinogenesis. Cell, *103:* 481–490, 2000.
41. Bergers, G., Brekken, R., McMahon, G., Vu, T. H., Itoh, T., Tamaki, K., Tanzawa, K., Thorpe, P., Itohara, S., Werb, Z., and Hanahan, D. Matrix metalloproteinase-9 triggers the angiogenic switch during carcinogenesis. Nat. Cell Biol., *2:* 737–744, 2000.
42. Vu, T. H., Shipley, J. M., Bergers, G., Berger, J. E., Helms, J. A., Hanahan, D., Shapiro, S. D., Senior, R. M., and Werb, Z. MMP-9/gelatinase B is a key regulator of growth plate angiogenesis and apoptosis of hypertrophic chondrocytes. Cell, *93:* 411–422, 1998.
43. Rabbani, S. A., and Mazar, A. P. The role of the plasminogen activation system in angiogenesis and metastasis. Surg. Oncol. Clin. N. Am., *10:* 393–415, 2001.
44. Kjoller, L. The urokinase plasminogen activator receptor in the regulation of the actin cytoskeleton and cell motility. J. Biol. Chem., *383:* 5–19, 2002.
45. Chapman, H. A., and Wei, Y. Protease crosstalk with integrins: the urokinase receptor paradigm. Thromb. Haemost., *86:* 124–129, 2001.
46. Clezardin, P. Recent insights into the role of integrins in cancer metastasis. Cell Mol. Life Sci., *54:* 541–548, 1998.
47. Lund, L. R., Romer, J., Bugge, T. H., Nielsen, B. S., Frandsen, T. L., Degen, J. L., Stephens, R. W., and Dano, K. Functional overlap between two classes of matrix-degrading proteases in wound healing. EMBO J., *18:* 4645–4656, 1999.
48. Vlachaki, M., Hernandez-Garcia, A., Ittmann, M., Chhikara, M., Aguilar, L., Zhu, Z., The, B., Butler, E., Woo, S., Thompson, T., Barrera-Saldana, H., and Aguilar-Cordova, E. Impact of preimmunization on adenoviral vector expression and toxicity in a subcutaneous mouse cancer model. Mol. Ther., *6:* 342–348, 2002.